

Prostate Specific Antigen Biosensor Based on Long Range Surface Plasmon-Enhanced Fluorescence Spectroscopy and Dextran Hydrogel Binding Matrix

Yi Wang,^{†,*} Annette Brunsen,[‡] Ulrich Jonas,^{‡,§} Jakub Dostálek,^{*,†} and Wolfgang Knoll[†]

Austrian Institute of Technology, Donau-City-Strasse 1, 1220 Vienna, Austria, Max-Planck Institute for Polymer Research, Ackermannweg 10, 55128 Mainz, Germany, and Foundation for Research and Technology, Institute of Electronic Structure and Laser (FORTH/IESL), Voutes 1527, 71110 Heraklion, Greece

A new biosensor based on surface plasmon-enhanced fluorescence spectroscopy (SPFS), which employs long-range surface plasmons (LRSP) and a photo-cross-linkable carboxymethyl dextran (PCDM) hydrogel binding matrix, is reported. LRSPs are surface plasmon modes that propagate along a thin metallic film with orders of magnitude lower damping compared to regular surface plasmons. Therefore, their excitation provides strong enhancement of the intensity of the electromagnetic field and a greatly increased fluorescence signal measured upon binding of fluorophore-labeled molecules on the sensor surface. In addition, these modes exhibit highly extended evanescent fields penetrating up to micrometers in distance from the metallic sensor surface. Therefore, a PCDM hydrogel with approximately micrometer thickness was anchored on the sensor surface to serve as the binding matrix. We show that this approach provides large binding capacity and allows for the ultrasensitive detection. In a model experiment, the developed biosensor platform was applied for the detection of free prostate specific antigen (f-PSA) in buffer and human serum by using a sandwich immunoassay. The limit of detection at the low femtomolar range was achieved, which is approximately 4 orders of magnitude lower than that for direct detection of f-PSA based on the monitoring of binding-induced refractive index changes.

Surface plasmon resonance (SPR) biosensors become an important technology that is pushed forward for rapid and sensitive detection of chemical and biological species.¹ In this method, the analyzed liquid sample is flowed over a metallic sensor surface with attached biomolecular recognition elements. The capture of target molecules on a sensor surface is probed by resonantly excited surface plasmons (SPs) and the binding-induced changes in the refractive index are detected. SPR biosensors offer the advantage of direct detection of biomolecular binding events. For medium size proteins such as prostate specific

antigen (PSA), SPR biosensors were shown to allow the direct detection at concentrations in the nanomolar range for which the molecular binding induces sufficiently large refractive index changes.^{2,3} However, such sensitivity is often not sufficient in many applications and thus approaches for enhancing the refractive index changes were investigated. These include the assays with metallic nanoparticle^{4–7} and enzyme⁸ labels, which were demonstrated to improve the limit of detection (LOD) by several orders of magnitude. In addition, an approach for advancing the sensitivity through the combining of SPR biosensors with fluorescence spectroscopy was developed.^{9,10} In this method, referred to as surface plasmon-enhanced fluorescence spectroscopy (SPFS), the capture of molecules labeled with fluorophores is observed through the detection of the intensity of the fluorescence light emitted from the sensor surface. This technique takes advantage of the strong intensity of the electromagnetic field accompanied with the resonant excitation of surface plasmons. The interaction of fluorophores with the evanescent field of surface plasmons allows for enhancing the excitation rate¹¹ of molecules adhered to the metallic surface as well as for the efficient collection of the fluorescence light.¹² SPFS biosensors that rely on immunoassays were shown to enable the detection of protein molecules below femtomolar concentrations.¹³

- (2) Cao, C.; Kim, J. P.; Kim, B. W.; Chae, H.; Yoon, H. C.; Yang, S. S.; Sim, S. J. *Biosens. Bioelectron.* **2006**, *21*, 2106–2113.
- (3) Huang, L.; Reekmans, G.; Saerens, D.; Friedt, J. M.; Frederix, F.; Francis, L.; Muyldermans, S.; Campitelli, A.; Van Hoof, C. *Biosens. Bioelectron.* **2005**, *21*, 483–490.
- (4) Wark, A. W.; Lee, H. J.; Qavi, A. J.; Corn, R. M. *Anal. Chem.* **2007**, *79*, 6697–6701.
- (5) Lee, H. J.; Wark, A. W.; Corn, R. M. *Analyst* **2008**, *133*, 596–601.
- (6) Mitchell, J. S.; Wu, Y. Q.; Cook, C. J.; Main, L. *Anal. Biochem.* **2005**, *343*, 125–135.
- (7) He, L.; Musick, M. D.; Nicewarner, S. R.; Salinas, F. G.; Benkovic, S. J.; Natan, M. J.; Keating, C. D. *J. Am. Chem. Soc.* **2000**, *122*, 9071–9077.
- (8) Goodrich, T. T.; Lee, H. J.; Corn, R. M. *J. Am. Chem. Soc.* **2004**, *126*, 4086–4087.
- (9) Dostalek, J.; Knoll, W. *Biointerphases* **2008**, *3*, FD12–FD22.
- (10) Neumann, T.; Johansson, M. L.; Kambhampati, D.; Knoll, W. *Adv. Funct. Mater.* **2002**, *12*, 575–586.
- (11) Liebermann, T.; Knoll, W. *Colloids Surf. A: Physicochem. Eng. Aspects* **2000**, *171*, 115–130.
- (12) Matveeva, E.; Gryczynski, Z.; Gryczynski, I.; Malicka, J.; Lakowicz, J. R. *Anal. Chem.* **2004**, *76*, 6287–6292.
- (13) Yu, F.; Persson, B.; Lofas, S.; Knoll, W. *J. Am. Chem. Soc.* **2004**, *126*, 8902–8903.

* Corresponding author. E-mail: jakub.dostalek@ait.ac.at. Fax: +43 50550 4399.

[†] Austrian Institute of Technology.

[‡] Max-Planck Institute for Polymer Research.

[§] FORTH/IESL.

(1) Homola, J. *Chem. Rev.* **2008**, *108*, 462–493.

Recently, long-range surface plasmons (LRSPs) were exploited for SPFS biosensing.^{14–16} These optical waves originate from the coupling of surface plasmons on opposite surfaces of a thin metallic film that is embedded between dielectrics with similar refractive indices. LRSPs exhibit orders of magnitude lower damping compared to regular surface plasmons on an individual metallic surface.¹⁷ Therefore, their excitation provides larger enhancement of the electromagnetic field intensity and thus allows for a stronger increase in the fluorescence signal in SPFS sensors. In addition, LRSPs probe the medium adjacent to the metallic surface with more extended evanescent field than regular surface plasmons.¹⁵ Therefore, three-dimensional binding matrixes with up to a micrometer thickness have been proposed for the immobilization of biomolecular recognition elements with large surface density that allows one to exploit the whole evanescent field of LRSP.¹⁸ Currently, new hydrogels materials based on NIPAAm [*N*-(isopropylacrylamide)] and dextran polymers were developed in our laboratory and they were demonstrated to be suitable for the construction of such surface architectures.^{19–21}

We report a new ultrasensitive biosensor exploiting LRSP-enhanced fluorescence spectroscopy with photo-cross-linkable carboxymethyl dextran (PCMD) hydrogel binding matrix for the detection of prostate specific antigen (PSA) in human serum. PSA is a 33–34 kDa single-chain glycoprotein which has been used for the diagnosis of prostate cancer.²² The analyte is present in blood serum in the form of free PSA (f-PSA) and PSA bound to antichymotrypsin (PSA-ACT). Currently, clinically relevant levels of this analyte in blood serum are below 0.3 nM (corresponding to 10 ng mL⁻¹) and they are routinely analyzed in specialized laboratories by, e.g., enzyme-linked immunosorbent assays (ELISA).²³ Biosensors for rapid detection of PSA at orders of magnitude lower concentrations are expected to provide a valuable tool for point-of-care diagnosis (POC) of female breast cancer,²⁴ for early identification of prostate cancer relapse,²⁵ and in forensic applications.²⁶ Research in novel methods for ultrasensitive and simplified analysis of PSA was carried out including immuno-PCR (LOD of 6 fM and analysis time >150 min),²⁷ bio barcode-based detection (LOD of 30 aM and analysis time of 80 min),²⁸ gold nanoparticle sandwich immu-

noassay combined with surface-enhanced Raman scattering (SERS) (LOD of 30 fM and analysis time of ~550 min)²⁹ and SPR (LOD of 30 pM)³ and SPFS with sandwich immunoassay (LOD of 80 fM and analysis time of 40 min).³⁰

MATERIALS AND METHODS

Chemicals and Biochemicals. All reagents were used as received without further purification. f-PSA (>95% pure from human seminal fluid, A32874H), a monoclonal mouse IgG₁ antibody recognizing the PSA epitope 4 used as a capture antibody (c-Ab, M86599M), and a monoclonal mouse IgG_{2a} antibody specific for the PSA epitope 6 used as a detection antibody (d-Ab, M86506M) were obtained from Biodesign (Biosite, Sweden). HBS-EP buffer (degassed 10 mM HEPES buffered saline, pH 7.4, 150 mM NaCl, 3 mM EDTA, 0.005% (v/v) surfactant P-20), acetate buffer (10 mM, pH 5.0), and glycine buffer (10 mM, pH 1.7) were obtained from Biacore (Sweden). The d-Ab was labeled by using an Alexa Fluor 647 labeling kit from Molecular Probes Inc.. The dye-to-protein molar ratio was determined by an UV–visible spectrometer as 5. Single donor female serum was obtained from Innovative Research. The novel photo-cross-linkable carboxymethyl dextran (PCMD) was synthesized as described in detail by Brunsen et al.³¹ Briefly, 10 g of dextran (MR ~ 2 000 000 from Sigma Aldrich) was dissolved in 150 mL of distilled water followed by the addition of 20 g (0.21 mol) of sodium chloroacetate (Acros Organics). In order to initiate the reaction, 50 mL of 8 M sodium hydroxide solution was added and the reaction was carried out for 1 h at the temperature of 62 °C. After the mixture was cooled down for 10 min, the reaction was terminated by neutralizing with 6 M hydrochloric acid. The carboxymethylated dextran (CMD) was precipitated in ice cold ethanol and purified by dialyzing against distilled water. After evaporation of the solvent, CMD is obtained as a white powder. For the benzophenone coupling, 1 g of CMD was dissolved in dried DMSO and kept under argon atmosphere. The reaction was carried for 3 h at room temperature after the addition of 0.35 g (0.00166 mol) of TFA-NHS and ~5 mL of 4-methylmorpholine (Merck). The obtained mixture was dialyzed against DMSO overnight and was directly followed by the reaction with 0.4 g (0.0019 mol)/0.22 g (0.000 95 mol) 4-aminomethylbenzophenone in DMSO with 5 mL/10 mL of 4-methylmorpholine at room temperature and under argon atmosphere. The obtained compound was purified by extensive dialyzing against DMSO and distilled water. As seen in Figure 1, the PCMD carried carboxylic groups for the anchoring of protein molecules via their amino groups and benzophenone groups for the cross-linking and attaching of the gel to a metallic surface that was modified with benzophenone moieties by UV light. In the following experiments, we used two PCMDs with the ratio of benzophenone and carboxylic groups to C–H groups of 1:6.5:34 and 1:4.4:23, respectively. The benzophenone-terminated thiol was synthesized at the Max Planck Institute for Polymer Research in Mainz, as described previously.²⁰

- (14) Kasry, A.; Knoll, W. *Appl. Phys. Lett.* **2006**, *89*, 101106.
 (15) Dostalek, J.; Kasry, A.; Knoll, W. *Plasmonics* **2007**, *2*, 97–106.
 (16) Wang, Y.; Dostalek, J.; Knoll, W. *Biosens. Bioelectron.* **2009**, *24*, 2264–2267.
 (17) Sarid, D. *Phys. Rev. Lett.* **1981**, *47*, 1927–1930.
 (18) Kasry, A.; Dostalek, J.; Knoll, W. In *Advanced Surface Design for Biomaterial and Life Science Applications*; Jenkins, A. T. A., Foersch, R., Schoenherr, H., Eds.; Wiley-VCH: Weinheim, Germany, 2009; pp 447–460.
 (19) Aulasevich, A.; Roskamp, R. F.; Jonas, U.; Menges, B.; Dostalek, J.; Knoll, W. *Macromol. Rapid Commun.* **2009**, *30*, 872–877.
 (20) Beines, P. W.; Klosterkamp, I.; Menges, B.; Jonas, U.; Knoll, W. *Langmuir* **2007**, *23*, 2231–2238.
 (21) Knoll, W.; Kasry, A.; Yu, F.; Wang, Y.; Brunsen, A.; Dostalek, J. *J. Nonlinear Opt. Phys. Mater.* **2008**, *17*, 121–129.
 (22) Watt, K. W.; Lee, P. J.; M'Timkulu, T.; Chan, W. P.; Loor, R. *Proc. Natl. Acad. Sci. U.S.A.* **1986**, *83*, 3166–3170.
 (23) Acevedo, B.; Perera, Y.; Ruiz, M.; Rojas, G.; Benitez, J.; Ayala, M.; Gavilondo, J. *Clin. Chim. Acta* **2002**, *317*, 55–63.
 (24) Radowicki, S.; Kunicki, M.; Bandurska-Stankiewicz, E. *Eur. J. Obstet. Gynecol. Reprod. Biol.* **2008**, *138*, 212–216.
 (25) Doherty, A. P.; Bower, M.; Smith, G. L.; Miano, R.; Mannion, E. M.; Mitchell, H.; Christmas, T. J. *Br. J. Cancer* **2000**, *83*, 1432–1436.
 (26) Johnson, E. D.; Kotowski, T. M. *J. Forensic Sci.* **1993**, *38*, 250–258.
 (27) Lind, K.; Kubista, M. *J. Immunol. Methods* **2005**, *304*, 107–116.
 (28) Nam, J. M.; Thaxton, C. S.; Mirkin, C. A. *Science* **2003**, *301*, 1884–1886.

(29) Grubisha, D. S.; Lipert, R. J.; Park, H. Y.; Driskell, J.; Porter, M. D. *Anal. Chem.* **2003**, *75*, 5936–5943.

(30) Yu, F.; Persson, B.; Lofas, S.; Knoll, W. *Anal. Chem.* **2004**, *76*, 6765–6770.

(31) Brunsen, A.; Jonas, U.; Dostalek, J.; Menges, B.; Knoll, W. Manuscript in preparation.

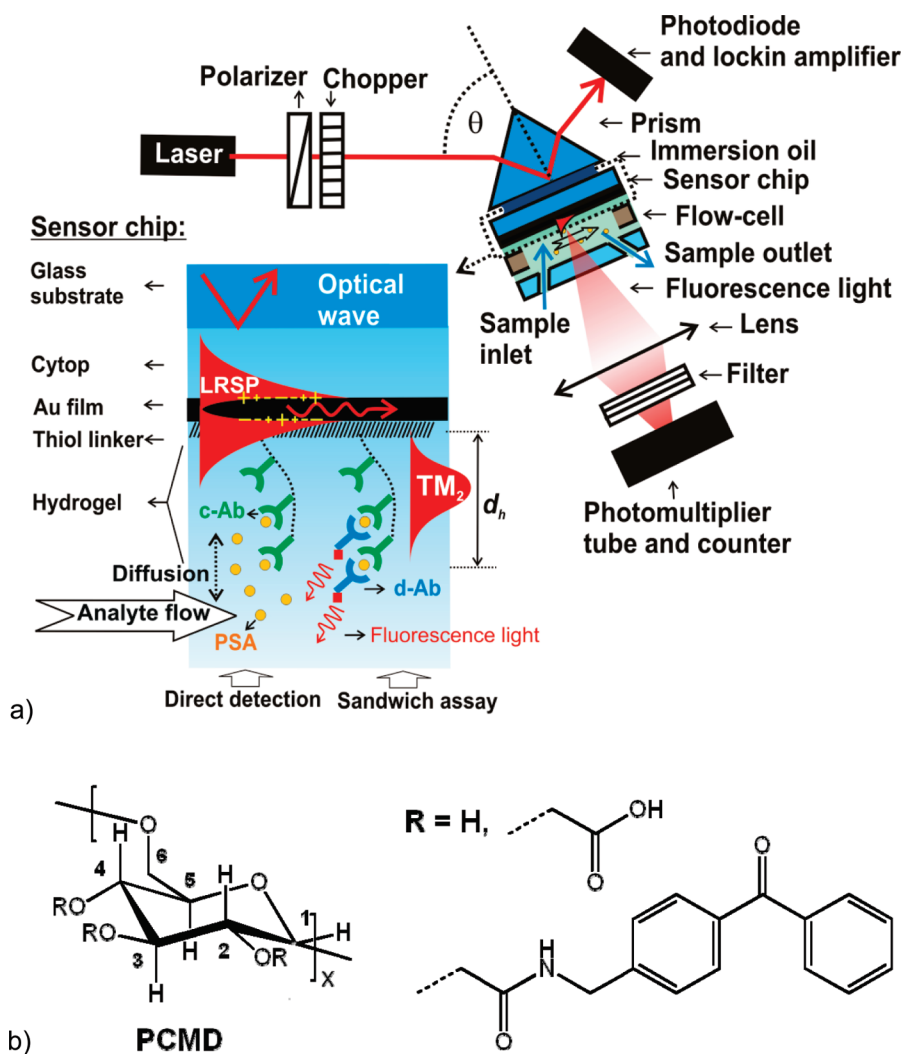


Figure 1. (a) Scheme of the optical setup for the excitation of LRSPs on the sensor surface with PCMD hydrogel binding matrix and the f-PSA detection immunoassays and (b) the PCMD chemical structure.

Sensor Instrument. As shown in Figure 1, an attenuated total reflection (ATR) method was used for the excitation of LRSPs on the sensor surface. A transverse magnetically (TM) polarized beam from a HeNe laser ($\lambda = 632.8$ nm) was coupled to a LASFN9 glass prism. Onto the prism base, a sensor chip with a layer structure supporting LRSPs was optically matched. This layer structure consisted of a low refractive index film (Cytop CTL-809 M obtained from ASAHI, Japan) and a gold film with the thicknesses of ~ 770 nm and ~ 20 nm, respectively, prepared as described previously.¹⁵ A flow-cell with a volume of approximately $12 \mu\text{L}$ was mounted against the sensor surface. Aqueous samples (with a refractive index close to $n_b = 1.333$) were pumped at the flow rate of 0.5 mL min^{-1} through the flow-cell using a peristaltic pump. The analyzed samples circulated in the fluidic system with a total volume of $800 \mu\text{L}$. The fluorescence light emitted from the sensor surface was collected through the flow-cell by a lens (numerical aperture $\text{NA} = 0.3$) and passed through a band-pass filter (transmission wavelength of $\lambda = 670$ nm); and its intensity was detected by a photomultiplier tube (PMT) from Hamamatsu (H6240-01, Japan). The LASFN9 glass prism was mounted on a motorized rotation stage, and angular reflectivity spectra $R(\theta)$ were measured by using a photodiode detector and lock-in amplifier. The monitoring of reflectivity

changes ΔR at an angle of incidence θ set to the maximum slope of the dip associated with the resonant excitation of LRSPs allowed the measurement of refractive index changes with the resolution around 10^{-6} refractive index units (RIU). The electronics supporting the sensor system was controlled by using the software Wasplas developed at the Max Planck Institute for Polymer Research in Mainz (Germany). The measured reflectivity curves were fitted by the transfer matrix-based model implemented in the software Winspall developed at the Max Planck Institute for Polymer Research in Mainz (Germany). With the use of this model, the thickness d_h and the refractive index n_h of the hydrogel binding matrix were determined by fitting the resonant angles for the excitation of LRSP and hydrogel waveguide modes similar as described before.¹⁹ In the further analysis, we assumed that the refractive index of the hydrogel n_h changes with the concentration of proteins and the hydrogel polymer as $\partial n/\partial c \approx 0.2 \mu\text{L mg}^{-1}$. From the refractive index contrast $n_h - n_b$ and the thickness d_h , the surface mass density Γ of the hydrogel film was calculated as

$$\Gamma = (n_h - n_b) d_h \frac{\partial c}{\partial n_h} \quad (1)$$

Functionalization of the Sensor Surface. The gold-coated substrates were immersed in ethanol containing 5 mM benzophenone-terminated thiol to allow the formation of a self-assembled monolayer (SAM). After the overnight incubation, the gold surface was rinsed with ethanol and dried with a nitrogen stream. On the surface modified by the thiol-SAM, a PCMD layer was deposited by spin-coating with the thickness in the range of 210–280 nm (measured in contact with air) from an aqueous solution with the concentration of PCMD between 60 and 80 mg mL⁻¹. Afterward, the PCMD film was dried at a temperature of $T = 45\text{ }^{\circ}\text{C}$ for 4 h and exposed to UV-light (wavelength of $\lambda = 254\text{ nm}$, irradiation energy dose of 2 J cm^{-2}) for 90 min in order to establish its photochemical attachment to the surface and cross-linking. Then, the substrates were mounted to the sensor, the PCMD hydrogel was swollen in ACT buffer at pH = 5, and in situ c-Ab were immobilized according to the following recipe. First, a mixture of 1-(3-dimethylaminopropyl)-3-ethylcarbodiimide hydrochloride (EDC, 37.5 mg mL⁻¹) and *N*-hydroxysuccinimide (NHS, 10.5 mg mL⁻¹) flowed for 8 min in order to form terminal NHS ester moieties. Afterward, the c-Ab dissolved in sodium acetate buffer (10 mM, pH 5.0) at a concentration of 50 $\mu\text{g mL}^{-1}$ was injected for 30 min followed by rinsing with ACT buffer for 10 min. The unreacted NHS ester moieties were deactivated by the incubation in a 1 M ethanolamine hydrochloride solution for 7 min.

Detection Assay. Series of samples were prepared by spiking HBS-EP buffer and human serum (volume of 800 μL) with f-PSA. Samples with f-PSA dissolved in HBS-EP at concentrations between 3 and 300 nM were used for the evaluation of the direct detection of f-PSA. For the SPFS-based detection, f-PSA was dissolved in human serum (with free PCMD at a concentration of 0.5 mg mL⁻¹) and HBS-EP buffer at concentrations ranging from 100 fM to 10 pM. In the direct detection experiment, HBS-EP buffer was flowed for 10 min in order to establish a baseline followed by an the incubation of the sensor surface with of a sample for 30 min and rinsing by HBS-EP buffer for 10 min. Upon the binding of f-PSA to the PCMD hydrogel with c-Ab, the changes in reflectivity R were measured in time at a fixed angle θ set to the value providing the highest slope of the reflectivity LRSP dip. The direct sensor response was determined as the difference of the reflectivity signal ΔR before and after the f-PSA binding. In the SPFS-based detection, a sandwich immunoassay was employed. First, a sample spiked with f-PSA was flowed through the sensor cell for 15 min. Afterward, the hydrogel matrix was rinsed for 1 min with HBS-EP buffer and d-Ab dissolved at a concentration of 1 nM was flowed through the sensor cell for 10 min followed by rinsing with HBS-EP buffer for 5 min. The fluorescence signal F was measured as a function of time at the resonant angle of incidence θ providing strong enhancement of the electromagnetic field due to the coupling to LRSPs. The fluorescence sensor response ΔF was evaluated as the difference between the fluorescence signal F before the injection of d-Ab and after the 4.5 min washout with HBS-EP (data points measured during 1 min were averaged). The detection was performed in cycles. After each detection cycle, the sensor surface was regenerated by a 5–10 min pulse of glycine (pH = 1.5) and a 5–15 min

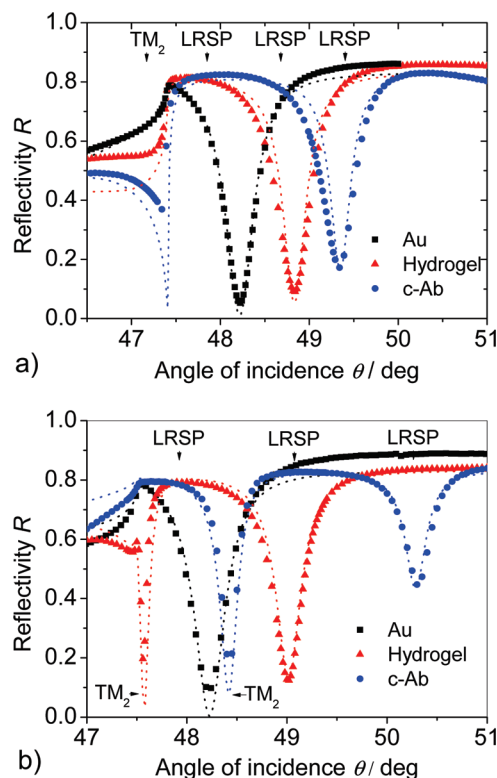


Figure 2. Angular reflectivity spectra for a hydrogel film (a) with the ratio of benzophenone to C–H groups of 1:34 and the thickness of 210 nm (measured in the contact with the air) and (b) with the ratio of benzophenone to C–H groups of 1:23 and the thickness of 280 nm (measured in the contact with the air). The \blacksquare show the spectra for the bare gold surface, \blacktriangle show the spectra measured after the attaching and swelling of the gel, and \bullet show the spectra measured after the immobilization of c-Ab (HBS-EP buffer was flowed along the sensor surface). The dotted lines show the corresponding fits of measured reflectivity curves.

pulse of 10 mM NaOH in order to release the captured f-PSA leaving free c-Ab binding sites.

RESULTS AND DISCUSSION

Swelling Properties. First, the swelling properties of the PCMD hydrogel were evaluated. Figure 2 shows the reflectivity spectra measured for the bare gold surface, for the swollen hydrogel film attached to the gold surface, and for the swollen hydrogel modified by the capture antibody c-Ab. These data reveal that after the attachment of the hydrogel film and its swelling in HBS-EP buffer, the resonance dip associated with the excitation of LRSP shifts to higher angles with respect to that on a bare gold surface. In addition, the reflectivity curve is changed in the vicinity of the critical angle $\theta = 47.5^{\circ}$ due to the appearance of an optical waveguide mode TM_2 supported by the thin hydrogel layer. In Figure 2a, reflectivity curves measured for the hydrogel film with the ratio of benzophenone to C–H group of 1:34 and thickness of $d_h = 210\text{ nm}$ (in contact with air) are shown. The spectrum measured was fitted after the swelling of the gel in HBS-EP buffer, and its thickness and refractive index was determined as $d_h = 0.98\text{ }\mu\text{m}$ and $n_h = 1.346$. On the basis of the effective medium theory,³² we determined the polymer volume fraction as $f = 7\%$ by using the equation:

(32) Aspnes, D. E. *Thin Solid Films* **1982**, 89, 249–262.

$$f = \frac{(n_h^2 - n_b^2)(n_{h\text{-dry}}^2 + 2n_b^2)}{(n_h^2 + 2n_b^2)(n_{h\text{-dry}}^2 - n_b^2)} \quad (2)$$

where $n_{h\text{-dry}} = 1.51^{33}$ is the refractive index of dry dextran polymer. Figure 2b shows the reflectivity curves for the hydrogel with the higher ratio of benzophenone to C–H groups of 1:23 that was deposited with a higher thickness $d_h = 280$ nm (in contact with air). The fitting of the respective angular reflectivity spectra measured after the swelling in HBS-EP revealed that it exhibited larger thickness of $d_h = 1.3 \mu\text{m}$ and a higher refractive index $n_h = 1.352$ corresponding to a polymer volume fraction around 10%. Let us note that the optical thickness of this gel was high enough to support a TM_2 mode as can be seen from the additional resonance dip located at the angle of incidence $\theta = 47.6$. Surface mass densities of $\Gamma = 59$ and 117 ng mm^{-2} were determined for two hydrogel films with a thickness in the swollen state of $d_h = 0.98$ and $1.3 \mu\text{m}$, respectively (measured in HBS-EP buffer). These data indicate that the higher concentration of benzophenone groups resulted in a higher gel density in the swollen state. The immobilization of a capture antibody c-Ab into the hydrogel layer caused an increase in the refractive index of the gel as seen from the shifts of the resonant dips due to the excitation of the LRSPs and TM_2 hydrogel waveguide modes. The fitting of the corresponding reflectivity spectra indicate that the refractive index increased to $n_h = 1.355$ and 1.372 for the hydrogels with a thickness of $d_h = 0.98$ and $1.3 \mu\text{m}$, respectively, and that the thickness of the hydrogel films swollen in HBS-EP buffer did not change significantly. The surface mass density of the thicker hydrogel film ($d_h = 1.3 \mu\text{m}$) and of the thinner film ($d_h = 0.98 \mu\text{m}$) increased to $\Gamma = 247 \text{ ng mm}^{-2}$ and $\Gamma = 103 \text{ ng mm}^{-2}$, respectively. The amount of anchored c-Ab molecules was estimated as the difference between the surface mass density before and after the c-Ab coupling as $\Gamma = 130$ and 44 ng mm^{-2} for the thicker and thinner films, respectively, that is up to order of magnitude higher than that reported for regularly used dextran brush exhibiting the thickness of about 100 nm (CM5 chip from Biacore, Sweden).³⁴ The prepared dextran hydrogel surfaces allowed for the immobilization of a large amount of c-Ab of which the surface mass density was close to that of the PCMD gel itself. In further experiments, we used the hydrogel with lower volume fraction around 7%.

Kinetic Analysis of the Affinity Binding in the Hydrogel Matrix. The affinity binding of f-PSA to the c-Ab receptors immobilized in a PCMD hydrogel was observed by LRSP spectroscopy and by LRSP-enhanced fluorescence spectroscopy. In the following experiment, we used a hydrogel with the thickness and surface mass density of $d_h = 0.95$ and $\Gamma = 66.5 \text{ ng mm}^{-2}$, respectively, measured prior to the modification by c-Ab. The gel was modified by c-Ab with the surface mass density of $\Gamma = 48 \text{ ng mm}^{-2}$. First, HBS-EP buffer was flowed over the sensor surface in order to establish a baseline of the reflectivity signal

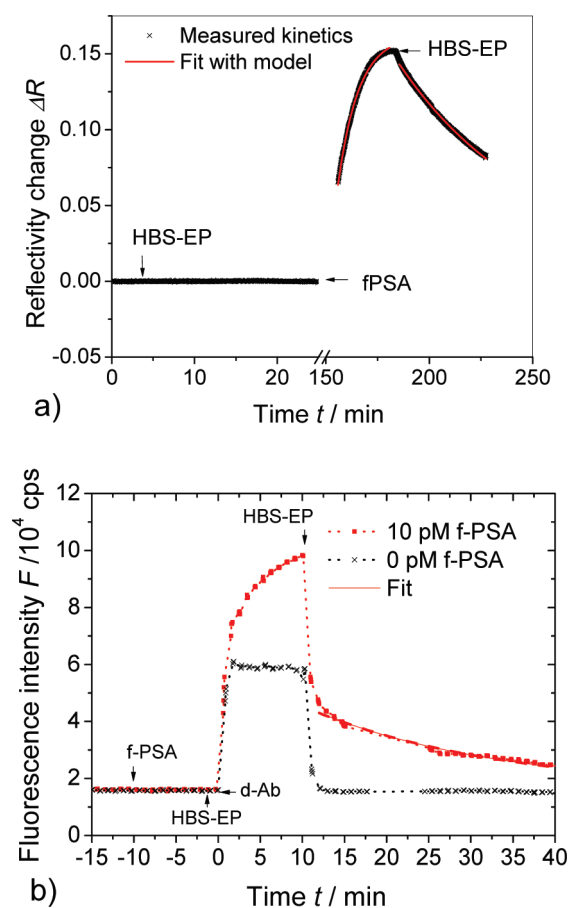


Figure 3. (a) Time evolution of the reflectivity changes ΔR upon the dissociation and association of f-PSA to c-Ab. The concentration of f-PSA in HBS-EP was 300 nM, and the c-Ab was immobilized with surface mass density of $\Gamma = 48 \text{ ng mm}^{-2}$ in the gel with the thickness of $d_h = 950 \text{ nm}$ (measured in HBS-EP). (b) Fluorescence signal measured upon the successive flow of a solution with f-PSA (concentration of 10 pM in HBS-EP) and Alexa Fluor 647 chromophore-labeled d-Ab (dissolved concentration of 1 nM in HBS-EP).

ΔR . Afterward, a solution with f-PSA dissolved at a concentration of 300 nM was injected for 30 min and a gradual increase in the reflectivity was observed due to the refractive index changes induced by f-PSA binding, see Figure 3a. After this association phase, HBS-EP buffer was flowed through the sensor cell and an exponential decrease in the reflectivity R was observed due to the dissociation of the f-PSA from c-Ab. With the measured kinetics fitted with a Langmuir adsorption model,³⁵ the association and dissociation constants were determined as $k_a = 4.8 \times 10^3 \text{ M}^{-1} \text{ s}^{-1}$ and $k_d = 2.4 \times 10^{-4} \text{ s}^{-1}$, respectively. These values are comparable to those reported by Yu et al. ($k_a = 2.2 \times 10^4 \text{ M}^{-1} \text{ s}^{-1}$ and $k_d = 3.2 \times 10^{-4} \text{ s}^{-1}$)³⁰ who analyzed the identical antigen–antibody pair by a SPR biosensor with c-Ab immobilized with a surface mass density of $\Gamma = 1.8 \text{ ng mm}^{-2}$ on the CM5 chip coated by a dextran brush (from Biacore, Sweden). The approximately 4-fold lower association constant k_a indicates that the diffusion of f-PSA through the PCMD hydrogel highly loaded with c-Ab did not hinder the binding kinetics dramatically. Moreover, we observed the affinity

(33) Piehler, J.; Brecht, A.; Hehl, K.; Gauglitz, G. *Colloids Surf., B* **1999**, *13*, 325–336.

(34) Lofas, S.; Johnsson, B.; Edstrom, A.; Hansson, G.; Linquist, G.; Muller, R.; Stigh, L. *Biosens. Bioelectron.* **1995**, *10*, 813–822.

(35) Schuck, P. *Annu. Rev. Biophys. Biomol. Struct.* **1997**, *26*, 541–566.

binding of the detection antibody d-Ab labeled with Alexa-Fluor 647 chromophore to the captured f-PSA molecules by LRSP-enhanced fluorescence spectroscopy. Figure 3b shows the time kinetics of the fluorescence signal upon a 15 min flow of a solution with f-PSA dissolved at a concentration of 10 pM followed by a 2 min rinsing by HBS-EP buffer, 10 min flow of d-Ab at a concentration of 1 nM, and final rinsing by the HBS-EP buffer for 30 min. After the time $t = 0$ when the d-Ab solution was injected, an increase in the fluorescence signal is observed due to the diffusion of d-Ab molecules into the gel and the affinity binding to the captured f-PSA molecules. During the flow of the HBS-EP buffer for time $t > 10$ min, a fast drop of the fluorescence signal F is observed owing to the washout of unbound d-Ab molecules. Afterward, the fluorescence signal exponentially decreased due to the dissociation of the complex c-Ab/f-PSA/d-Ab. By fitting the exponential decay of the signal with the Langmuir model, we determined the dissociation constant as $k_d = 5.5 \times 10^{-4} \text{ s}^{-1}$. This value is comparable to that measured for the dissociation of the f-PSA bound to c-Ab which indicates good stability of c-Ab, f-PSA, and the d-Ab complex.

Direct Detection of f-PSA. With the use of spectroscopy of LRSPs and a hydrogel matrix with thickness $d_h = 950 \text{ nm}$ and surface mass density of $\Gamma = 66.5 \text{ ng mm}^{-2}$, direct detection of f-PSA in HBS-EP buffer was performed. As shown in Figure 4a, the sequential injection of samples with f-PSA at concentrations between 3 and 300 nM induced a gradual increase in the reflectivity ΔR . After the injection of the sample with the maximum f-PSA concentration of 300 nM, the increase in the reflectivity shift ΔR started to saturate and reached the approximate value $\Delta R = 0.16$. The specificity of the f-PSA binding was verified in an experiment in which 30 nM f-PSA was flowed over the PCMD without c-Ab, which showed no significant change in the reflectivity (Figure 4a). In addition to the specific binding of f-PSA, we investigated the interaction of PCMD hydrogel with human serum that was not spiked with f-PSA. As seen in Figure 4b, upon the injection of a serum sample a large increase in the reflectivity change ΔR occurs which indicates that the blood serum efficiently diffuses inside the gel. After rinsing with HBS-EP for 5 min, the reflectivity stabilized at $\Delta R = 0.07$ above the original value prior to the incubation with serum. This change is due to the nonspecifically bound serum components adhering within the hydrogel matrix possibly due to electrostatic and physical adsorption. The nonspecifically bound serum can be fully washed out by applying the regeneration. In addition, the spiking of serum with free PCMD at a concentration of 0.5 mg mL^{-1} responded in an approximately 2.7-fold decrease of sensor response due to the adhered serum components. This behavior is similar to that in the dextran brush (CM5 chip from Biacore Inc., Sweden) reported by Yu et al.³⁰ and can be explained by the competitive binding of the substances contained in serum to free PCMD molecules, which reduces their adsorption within the gel. The calibration curve for the direct detection of f-PSA in HBS-EP buffer is presented in Figure 5. From these data, we determined a LOD of 0.68 nM as the concentration for which the linear fit of the calibration curve reaches 3 times the standard deviation of the baseline $3\sigma(\Delta R) = 8 \times 10^{-4}$.

Detection of f-PSA by SPFS. For the SPFS detection of f-PSA in HBS-EP buffer and human serum, a hydrogel with a thickness

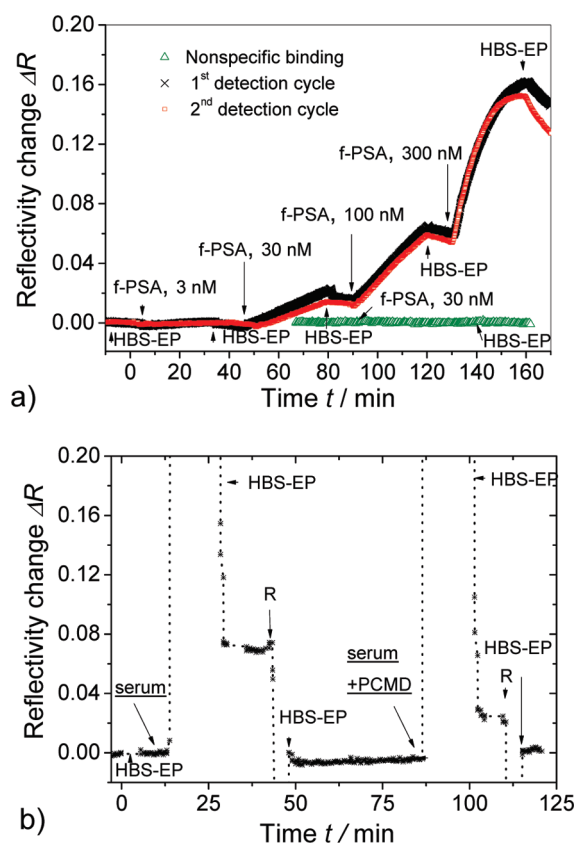


Figure 4. (a) Changes in the reflectivity ΔR measured upon the specific (\times and \square) and nonspecific (\triangle) binding of f-PSA dissolved at concentrations between 3 and 300 nM in the PCMD binding matrix. (b) Time evolution of the reflectivity changes ΔR for two detection cycles with the 15 min incubation in human serum with and without spiking with PCMD at the concentration of 0.5 mg mL^{-1} followed by the regeneration (R) and rinsing with HBS-EP buffer.

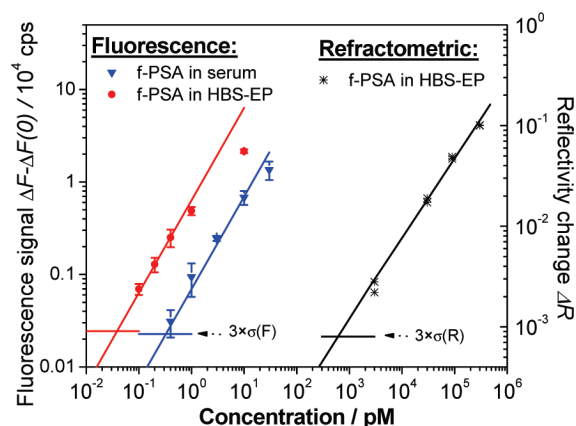


Figure 5. Calibration curves for the direct detection of f-PSA (refractometric, $*$) compared to the sandwich immunoassay-based detection with fluorescence readout for f-PSA dissolved in HBS-EP (\bullet) and in human serum (\blacktriangledown). The lines show the linear fit, and the error bars show the standard deviation.

of $d_h = 1.32 \text{ }\mu\text{m}$ and a surface mass density of $\Gamma = 56 \text{ ng mm}^{-2}$ was used. Into the gel, the capture antibody c-Ab was immobilized with a surface mass density of $\Gamma = 41 \text{ ng mm}^{-2}$. In these experiments, buffer and human serum samples spiked with f-PSA were analyzed. As described before, the analysis

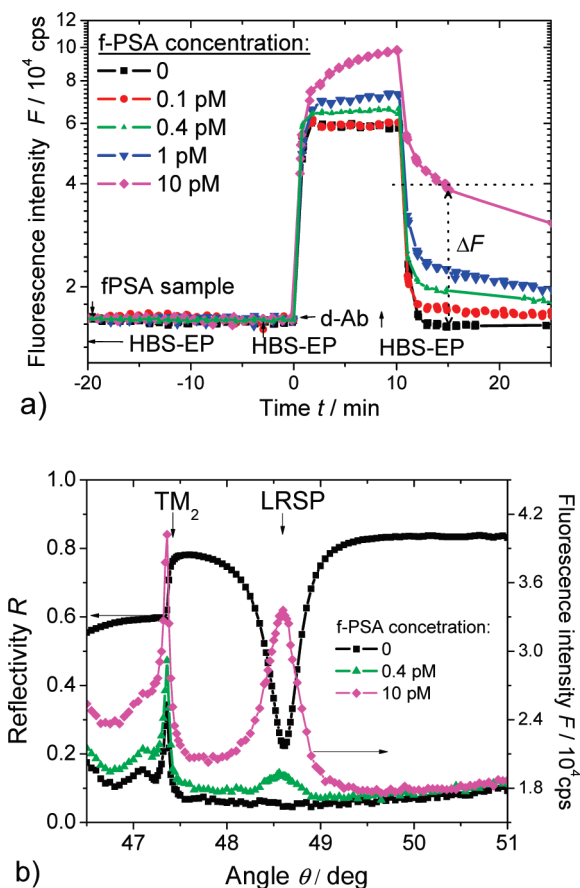


Figure 6. (a) Time evolution of the fluorescence signal F upon the analysis of HBS-EP samples spiked with f-PSA at concentrations 0–10 pM. (b) Angular fluorescence spectra measured after the flow of HBS-EP samples spiked with f-PSA at concentrations of 0, 0.4, and 10 pM.

was performed in cycles comprising the flow of the analyzed sample for 15 min followed by the 10 min incubation of the d-Ab, 5 min washout with HBS-EP buffer, and regeneration. Figure 6a shows the time evolution of the fluorescence signal F measured during the five detection cycles for the HBS-EP samples spiked with f-PSA at concentrations of 0–10 pM. These data reveal that fluorescence sensor response ΔF increases with the concentration of f-PSA. For the concentration of f-PSA equal to zero, a rapid steplike increase and decrease in the fluorescence signal F was observed at time $t = 0$ and 10 min, respectively, due to the diffusion of d-Ab in and out of the gel. No measurable change in the fluorescence signal ΔF was observed for the blank HBS-EP buffer sample, and the sample with the f-PSA at a concentration of 10 pM induced a sensor response of $\Delta F = 2.3 \times 10^4$ cps. After the flow of the detection antibody d-Ab, the angular fluorescence intensity spectra were measured for the concentrations of f-PSA 0, 0.4, and 10 pM, see Figure 6b. Strong fluorescence peaks were observed at the angle of incidence for which LRSPs were resonantly excited and their maximum intensity increases with the concentration of f-PSA. Moreover, an enhanced fluorescence signal was measured at angles close to the critical angle $\theta = 47.4^\circ$. This increase is due to the coupling of the incident light to the hydrogel waveguide mode TM_2 that provides an additional enhancement of the electromagnetic field intensity similar to LRSPs.

Similarly, we measured the sensor response ΔF for a series of human serum samples spiked with f-PSA. For the analysis of a blank human serum sample not spiked with f-PSA, a significant increase in the sensor response of $\Delta F(0) \sim 625$ cps was observed which was probably due to the nonspecific adsorption of d-Ab to the blood plasma components adhering to the sensor surface. The comparison of the calibration curve for the direct detection f-PSA in HBS-EP buffer (SPR) and for the fluorescence readout of sandwich immunoassay detection of f-PSA in HBS-EP and human serum (SPFS) is presented in Figure 5. The LOD for the SPFS readout was defined as the concentration for which the linear fit of the calibration curve reaches that for a blank sample $\Delta F(0)$ plus 3 times the standard deviation of the fluorescence signal $3\sigma(F) = 230$ cps. For the detection in HBS-EP buffer and human serum, the LOD of 34 and 330 fM was determined, respectively. The LOD of f-PSA in human serum is about 1 order of magnitude higher than that of f-PSA in buffer probably due to slower diffusion of f-PSA into the gel in the serum which exhibit higher viscosity and owing to the blocking the c-Ab antibody immobilized in the hydrogel matrix by means of nonspecific sorption. The sensor surface showed good reproducibility with the relative standard deviation of the sensor response ΔF of 4% after 30 detection cycles and 4 days of operation. SPFS-based analysis of an individual sample was performed in 30 min including the 15 min incubation of the sensor surface with a sample, 10 min flow of the d-Ab, and 5 min washout of the sensor surface. In comparison with the regular SPFS with dextran brush surface architecture reported by Yu et al.,³⁰ a moderate improvement of LOD (approximately 2-fold) and the sample incubation time (2-fold) was achieved. In human serum, the LOD was significantly deteriorated. This effect was probably due to the nonspecific interaction of the serum with the PCMD hydrogel matrix that was not observed for the dextran brush on the top of the CM5 chip (from Biacore, Sweden).

We expect that the LOD can be further improved by the optimization of the hydrogel density and thickness in order to provide faster diffusion of target analyte and its binding closer to the surface where the LRSP field enhancement is stronger. In addition, compacting the captured analyte on the sensor surface through externally triggered collapse observed for “smart” gels can be used for more sensitive detection of molecular binding.³⁶ For the thickness of the hydrogel matrix d_h larger than 1 μm , the excitation of an additional hydrogel waveguide mode was observed to provide enhancement of the fluorescence signal which may provide new, potentially more sensitive means for the detection of biomolecular binding events.

CONCLUSIONS

A new biosensor platform exploiting the excitation of long-range surface plasmons and a PCMD hydrogel binding matrix was developed and applied for the detection of f-PSA in human serum. The investigation of swelling properties of the PCMD hydrogel film with approximately micrometer thickness in the swollen state revealed that it exhibits a highly open structure in which protein catcher molecules can be immobilized with orders of magnitude larger surface mass density compared to, e.g., the monolayer surface architectures relying on thiol-SAM. The

(36) Huang, C. J.; Jonas, U.; Dostalek, J.; Knoll, W. *Proc. SPIE* **2009**, *7356*, 735625.

measurement of the kinetics of the binding of f-PSA to the immobilized catcher antibody showed that the target analyte can diffuse fast through the gel and the determined affinity binding constants were comparable to those obtained for other surface architectures. The direct detection of f-PSA by using the spectroscopy of LRSPs and sandwich immunoassay-based detection combined with SPFS were carried out. The LOD for the fluorescence-based detection of 34 fM was achieved in buffer, which was more than 4 orders of magnitude lower than that for the direct detection. In addition, the fluorescence readout combined with the sandwich immunoassay was less affected by the nonspecific interaction of human serum with the PCMD hydrogel matrix and allowed for the analysis of f-PSA at concentrations down to 330 fM. We expect that further optimization of the hydrogel matrix and modifying the optical scheme for the readout of arrays of sensing spots will provide a generic biosensor platform for rapid

and ultrasensitive analysis with potential applications in a range of important areas including medical diagnostics.

ACKNOWLEDGMENT

We gratefully acknowledge the financial support of the European Commission in the Communities sixth Framework Programme, Project TRACEBACK (Grant FOOD-CT-036300) coordinated by Tecnoalimenti. It reflects the author's views, and the Community is not liable for any use that may be made of the information contained in this publication. Partial support for this work was provided by Deutsche Forschungsgemeinschaft (Grant KN 224/18-1, Schwerpunktprogramm 1259 "Intelligente Hydrogele").

Received for review July 27, 2009. Accepted October 17, 2009.

AC901662E